Systems & Control Transactions

Research Article - Peer Reviewed Conference Proceeding
ESCAPE 35 - European Symposium on Computer Aided Process Engineering
Ghent, Belgium. 6-9 July 2025
Jan F.M. Van Impe, Grégoire Léonard, Satyajeet S. Bhonsale,
Monika E. Polańska, Filip Logist (Eds.)

PSE PRESS

A 2D Axisymmetric Transient State CFD Modelling of a Fixed-bed Reactor for Ammonia Synthesis

Leonardo Bravo[a], Camilo Rengifo[b], Martha Cobo[a], Manuel Figueredo[a]*

[a] Energy, Materials and Environment Laboratory, Faculty of Engineering, Universidad de La Sabana, Campus Universitario Puente del Común, Km. 7 Autopista Norte, Bogotá, Colombia.
[b] Department of Mathematics, Physics and Statistics, Universidad de La Sabana, Campus Universitario Puente del Común, Km. 7 Autopista Norte, Bogotá, Colombia.
* Corresponding Author: manuel.figueredo@unisabana.edu.co.

ABSTRACT

Power-to-Ammonia technology offers sustainable pathways for energy storage and chemical production, with fixed-bed reactors being critical components for efficient synthesis. Understanding reactor dynamics under varying conditions is essential for optimizing these systems, particularly when integrated with intermittent renewable energy sources. This study aims to develop and validate a 2D axisymmetric CFD model for analysing the dynamic response of a ruthenium-catalysed ammonia synthesis reactor to thermal perturbations. The model incorporates detailed reaction kinetics, multicomponent mass transport, and heat transfer mechanisms to predict system behaviour under transient conditions. Results reveal that a step increase in wall temperature from 400°C to 430°C enhances NH_3 concentration by 136% (from 2.2 to 5.1 vol.%), with rapid system stabilization achieved within 0.5 seconds. The thermals response maintains consistent heat transfer patterns, exhibiting ~400K differentials between inlet and maximum temperature zones

Keywords: Ammonia Synthesis, Process Intensification, Computational Fluid Dynamics, Alternative Fuels, Dynamic Modelling.

INTRODUCTION

Power-to-Ammonia (PtA) technology offers a sustainable and efficient solution by integrating renewable energy sources with carbon-neutral fuel production. This approach allows energy to be stored in the form of ammonia, which can serve as a fuel, energy carrier, or key ingredient in fertilizers [1]. The core of the PtA process lies in its reaction system, featuring a packed-bed reactor (PBR) where ammonia is synthesized from hydrogen (H_2) produced via water electrolysis and nitrogen (N_2) captured from the atmosphere. Nevertheless, the synthesis process poses intricate multiscale challenges related to flow, heat, and mass transfer, largely driven by the highly exothermic nature of the reaction . Advanced modeling techniques, such as Computational Fluid Dynamics (CFD), are essential to address these challenges, enabling optimization of reactor performance, catalyst utilization, and overall energy efficiency [2].

Several studies have focused on CFD simulation of the PBR reactor in steady state. Gu et al. [4] explored decentralized ammonia synthesis for hydrogen storage and transport using a CFD model, focusing on a small-scale Haber-Bosch reactor with Ruthenium-based catalysts optimized for mild conditions. The model's accuracy was validated against experimental data and parametric studies were conducted to assess the impact of key operational parameters. The results showed that temperature is the most influential factor affecting ammonia production and pressure primarily affects the chemical equilibrium. Furthermore, the study identified an optimal gas hourly space velocity (GHSV) of 1.8·10^5 h^(-1) for efficient ammonia synthesis. Nikzad et al. [5] compared the performance of three different reactor configurations to find the optimal design to enhance nitrogen conversion and reduce pressure drops. The study used CFD simulations to analyze and compare the mass, energy and momentum conservation in a two-dimensional geometry of the three reactor types. The spherical reactors, particularly the spherical axial flow (SAF) configuration, were more efficient than conventional tubular reactors for

ammonia synthesis. Tyrański et al.[3] investigated the ammonia synthesis process in an axial-radial bed reactor using CFD focusing on understanding the influence of catalyst bed parameters, such as particle size and geometry modifications, on the efficiency of the reactor. The simulations demonstrated that smaller catalyst particles (1-2 mm) provided a higher ammonia formation rate, while larger particles show a slower reaction rate spread throughout the bed. Moreover, modifications in bed geometry could reduce the bed volume by half without losing efficiency.

However, in PtA systems, the intermittent nature of renewable energy sources, such as hydrogen production via electrolysis, introduces additional complexities in reactor performance. Boundary conditions and external disturbances, like variations in hydrogen flow or temperature fluctuations, can significantly impact key process variables, including reaction rates, heat transfer, and overall system stability. Therefore, understanding the reactor's transient response under such dynamic conditions is crucial.

This study focuses on developing a 2D axisymmetric transient CFD model for ammonia synthesis within a fixed-bed reactor, specifically analyzing the dynamic response to thermal perturbation at the reactor wall. By evaluating these transient states, the research aims to provide insights into reactor thermal behavior under temperature fluctuations that may occur in PtA systems.

MATHEMATICAL MODELING

Governing Equations

Table 1: Governing equations for the catalytic region.

Description	Mathematical Expression	Eq.
Transport of concentrated species	$\rho\frac{\partial\omega_i}{\partial t}+\nabla\cdot\mathbf{j_i}+\rho(\mathbf{u}\cdot\nabla)\omega_i=R_i$	(1)
	$\mathbf{j_i}=-\left(\rho D_i^m\nabla\omega_i+\rho\omega_i D_i^m\frac{\nabla M_n}{M_n}-\mathbf{j}_{c,i}\right)$	(2)
Heat transfer in porous media	$(\rho C_p)_{eff}\frac{\partial T}{\partial t}+\rho C_p\mathbf{u}\cdot\nabla T+\nabla\cdot\mathbf{q}=Q$	(3)
	$(\rho C_p)_{eff}=\theta_s\rho_s C_{p,s}+\epsilon_p\rho_f C_{p,f}$	(4)
	$\mathbf{q}=-k_{eff}\nabla T$	(5)
	$k_{eff}=\theta_s k_s+\epsilon_p k_f$	(6)
Brinkman-Forchheimer extended Darcy equation	$\frac{1}{\epsilon_p}\rho\frac{\partial\mathbf{u}}{\partial t}+\frac{1}{\epsilon_p}\rho(\mathbf{u}\cdot\nabla)\mathbf{u}\frac{1}{\epsilon_p}=\nabla\cdot[-p\mathbf{I}+\mathbf{K}]-\left(u\kappa^{-1}+\beta\epsilon_p\rho\lvert\mathbf{u}\rvert\right)\mathbf{u}$	(7)
	$\mathbf{K}=\mu\frac{1}{\epsilon_p}(\nabla\mathbf{u}+(\nabla\mathbf{u})^T-\frac{2}{3}\mu\frac{1}{\epsilon_p}(\nabla\cdot\mathbf{u})\mathbf{I}$	(8)
Continuity equation	$\frac{\partial\epsilon_p\rho}{\partial t}+\nabla\cdot(\rho\mathbf{u})=0$	(9)

Table 2: Governing equations for the free fluid region.

Description	Mathematical Expression	Eq.
Transport of concentrated species	$\rho\frac{\partial\omega_i}{\partial t}+\nabla\cdot\mathbf{j_i}+\rho(\mathbf{u}\cdot\nabla)\omega_i=0$	(10)
	$\mathbf{j_i}=-\left(\rho D_i^m\nabla\omega_i+\rho\omega_i D_i^m\frac{\nabla M_n}{M_n}-\mathbf{j}_{c,i}\right)$	(11)
Heat transfer in porous media	$\rho C_p\frac{\partial T}{\partial t}+\rho C_p\mathbf{u}\cdot\nabla T+\nabla\cdot\mathbf{q}=0$	(12)
	$\mathbf{q}=-k\nabla T$	(13)
Navier-Stokes equation	$\rho\frac{\partial\mathbf{u}}{\partial t}+\rho(\mathbf{u}\cdot\nabla)\mathbf{u}=\nabla\cdot[-p\mathbf{I}+\mathbf{K}],$	(14)
	$\mathbf{K}=\mu(\nabla\mathbf{u}+(\nabla\mathbf{u})^{\mathrm{T}})-\frac{2}{3}\mu(\nabla\cdot\mathbf{u})\mathbf{I}.$	(15)
Continuity equation	$\frac{\partial\rho}{\partial t}+\nabla\cdot(\rho\mathbf{u})=0$	(16)

The governing equations describing the behaviour of the fixed-bed reactor for ammonia synthesis can be divided into two main regions: the catalytic region and the free fluid region.

Kinetic Model for Ammonia Synthesis

The reaction follows a rate-limiting mechanism in which the dissociation of nitrogen is the lowest and most energy-intensive step. The overall reaction is represented as:

$$N_2(g)+3H_2(g)\rightarrow 2NH_3(g) \tag{17}$$

The reaction rate for ammonia synthesis on a ruthenium (Ru)-based catalyst is governed by a modified Temkin kinetic expression, which includes H_2 and NH_3 adsorption terms [4]. The rate expression is given by:

$$\frac{d\eta}{dt}=k\lambda(q)\left[\frac{(a_{N_2})^{0.5}\left[\frac{(a_{H_2})^{0.375}}{(a_{NH_3})^{0.25}}\right]-\frac{1}{Ka}\left[\frac{(a_{NH_3})^{0.75}}{(a_{H_2})^{1.125}}\right]}{1+K_{H_2}(a_{H_2})^{0.3}+K_{NH_3}(a_{NH_3})^{0.2}}\right] \tag{18}$$

The term $d\eta/dt$ represents the rate at which the limiting reactant is consumed, expressed in $mol\cdot h^{-1}\cdot dm_{cat}^3$. The kinetic constant for the reverse reaction (ammonia decomposition) is denoted as k, while K_a refers to the equilibrium constant for the reaction [5].The activities of the reactants and product are indicated by a_i. The stoichiometric coefficient, $\lambda(q)$, is set to 1 or 3 depending on whether the H_2/N_2 feed ratio is 3 or 1.5, respectively [6]. The absorption equilibrium constants of reactants K_{H_2} and K_{NH_3} are expressed by [7]. The activity of the ith species (NH_3, H_2 *or* N_2) a_i can be calculated as follows,

$$a_i=y_i\phi_i P \tag{19}$$

Where P indicates the total pressure (atm), y_i and ϕ_i denotate the mole fraction and fugacity coefficient of the ith species, respectively. The fugacity coefficients for the reactants and product are fitted by temperature (K) and

pressure (atm) using the equations in expressed by [5].

RESULTS AND DISCUSSION

Model Validation and Mesh Independence

A mesh independence study was conducted with four mesh configurations, as illustrated in Figure 1. The NH_3 production rate showed minimal variation between coarse (35.802 $kg \cdot m^{-3} \cdot s^{-1}$) and medium (35.825 $kg \cdot m^{-3} \cdot s^{-1}$) meshes (0.064% difference). The fine mesh (36.087 $kg \cdot m^{-3} \cdot s^{-1}$) was adopted, achieving an average element quality of 0.8155. Element quality, a dimensionless metric ranging from 0 to 1, evaluates the regularity of mesh element shapes, with values closer to 1 indicating optimal shape regularity and values near 0 signifying highly distorted or degenerated elements. This measure ensures numerical stability, geometric aligment, and computational accuracy. The selected mesh showed excellent agreement with experimental data from literature (35.5 – 36.5 $kg \cdot m^{-3} \cdot s^{-1}$) [7].

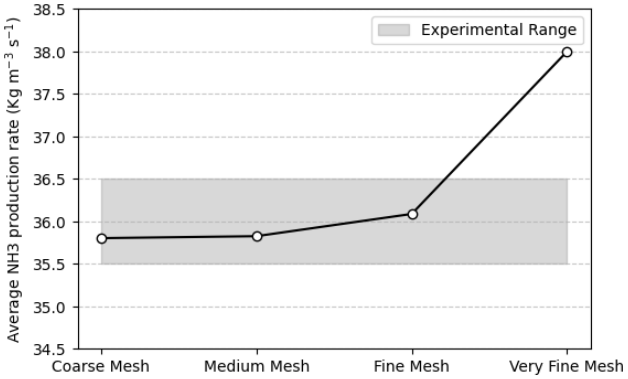

Figure 1: Effect of the mesh refinement on average NH_3 concentration under standard operating conditions (T=430 ℃, $P = 100$ bar, $GHSV = 180.000\ h^{-1}$).

Reaction Kinetic and Thermodynamic Response

The kinetic response to the wall temperature step change from 400℃ to 430℃ resulted in a rate constant enhancement factor of 2.08, as shown in Figure 2(a). The relative low activation energy of the Ru/C catalyst (23 kcal/mol) compared to traditional Fe-based catalyst (32 – 35 kcal/mol) accounts for this significant kinetic enhancement, explaining why the NH_3 concentration rapidly increased from 2.2 vol.% to 5.1 vol.% after the temperature perturbation. As shown in Figure 2(b), the equilibrium constant (Ka) decreased by approximately 35% at higher temperature, which thermodynamically favours the reverse reaction. However, the observed increase in NH_3 production (136%) demonstrates that the kinetic enhancement dominated over the equilibrium constraints in this temperature range. The surface chemistry evolution, depicted in Figure 2(c), shows that the absorption constants for both H_2 and NH_3 decreased with increasing temperature.

Thermal Dynamic Response Analysis

The dynamic behavior of the ammonia synthesis reactor under thermal disturbance was systematically investigated to evaluate its response to a step perturbation in the wall temperature. This analysis was conducted maintaining constant operating conditions of 70 bar pressure, GHSV of 180.000 h^{-1}, and H_2/N_2 feed ratio of 3.0, which represent steady-state operation parameters with the major production rates [7]. Figure 2(d) illustrates the magnitude of the wall temperature step, which was set to 30K based on the high sensitivity of Ru catalyst kinetics to temperature changes in this range, as demonstrated in previous studies [4], [6], [7]. This temperature step is also practically relevant, as it sits within the typical operating window (370-460℃) where Ru catalysts show high activity while avoiding excessive thermal stress on the reactor system.

NH_3 Production

The system's response to the temperature perturbation reveals significant insights into the reactor's dynamic behavior, Figure 2(d). Initially, the NH_3 concentration rapidly increases from 0 to approximately 2 vol.% during the first 0.5 seconds showing the system's quick response to the initial operating temperature of 400℃. This is followed by a brief stabilization period where the concentration remains steady at around 2.2 vol.%. At t = 1.0 s, when the step increase in temperature from 400℃ to 430℃ is implemented, the NH_3 concentration exhibits a sharp response, rising from 2.2 vol.% to approximately 5.1 vol.%. This dramatic increase, representing a 136% improvement in NH_3 production, demonstrates the strong temperature dependence of the reaction kinetics. The smooth transition and stable final concentration suggest that the reactor maintains operational stability despite the sudden temperature change, which is crucial for practical applications in industrial settings.

Thermal Distribution Evolution

The spatial temperature distributions before and after the step perturbation provide insights into the reactor's thermal behavior. Figure 3(a) shows the temperature field at t = 0.8 s, prior to the step change, where the wall temperature is maintained at 673.15 K (400℃). At this condition, the temperature ranges from 280 K at the inlet to 679 K near the reactor wall, displaying a significant thermal gradient characteristic of the exothermic ammonia synthesis process.

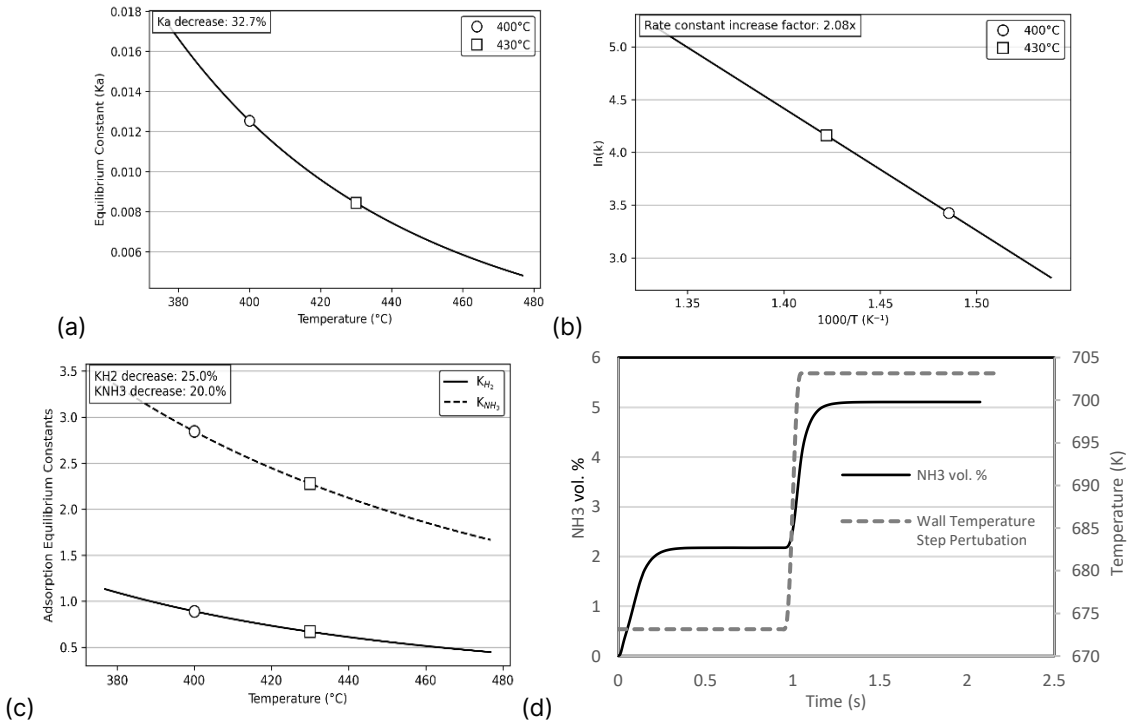

Figure 2: Thermal Dynamic Response of the Ammonia Synthesis Reactor. (a) Impact of temperature change on equilibrium constant. (b) Arrhenius behavior of NH_3 synthesis rate constant. (c) Temperature step change on adsorption constants. (d) Temperature step perturbation at the reactor walls and Dynamic respon of NH_3 volumetric concentration.

After the step perturbation (Figure 3(b), t = 2.0s), the system reaches a new thermal equilibrium with the elevated wall temperature of 703.15 K (430℃). The temperature distribution shows a similar pattern bit with higher overall values, ranging from 277 K at the inlet to 719 K in the reaction zone. The comparison between both states reveals that while the absolute temperatures have increased, the fundamental heat transfer characteristics remain consistent. The effective heat conduction through the catalyst bed is evidenced by the smooth temperature transitions, and the radial temperature distribution indicates significant wall-to-center heat transfer.

A notable observation is the persistence of steep temperature gradients near the inlet in both cases, with a temperature difference of approximately 400 K between the inlet and maximum temperature zones. This consistency in temperature differential, despite the step change in wall temperature, suggests robust heat transfer mechanisms within the reactor. The similarity in the thermal patterns before and after the perturbation indicates that the reactor design effectively manages heat distribution under changing thermal conditions, an essential characteristic for industrial applications where temperature fluctuations may occur.

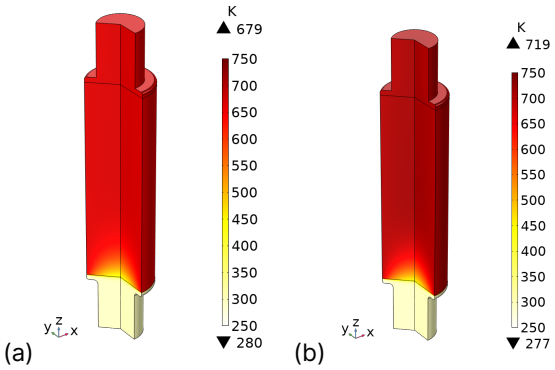

Figure 3. Temperature distribution in the reactor at (a) t = 0.8 s with wall temperature of 673.15 K (400℃) and (b) t = 2.0 s after step increase to 703.15 K (430℃).

NH_3 Concentration Evolution

The evolution of NH_3 concentration over time, as depicted in Figure 3, clearly represents the fixed-bed reactor's response to a step change in wall temperature, with critical phases occurring at t=0.9 s, t=0.9s, t=1.07 s, and t=2.0 s.

At t=0.9 s, Figure 4(a), prior to the temperature step

change, the wall temperature is maintained at 400°C. During this phase, localized ammonia formation is observed near the reaction zone. This reflects the catalytic activity at the steady-state baseline operating conditions, where the reactor exhibits a controlled and predictable NH_3 synthesis rate driven by the Ru/C catalyst's kinetics at the lower temperature.

At t=1.07 s, Figure 4(b), the step temperature change is introduced, rapidly elevating the wall temperature from 400°C to 430°C. This thermal perturbation triggers an immediate enhancement in the reaction rate, as the Ru/C catalyst demonstrates strong sensitivity to temperature increases. The resulting NH_3 concentration begins to expand radially, highlighting the acceleration of catalytic activity throughout the reactor. This phase represents the transitional behavior of the system as it responds dynamically to the external thermal input, aligning with the thermal response observed in Figure 1(b).

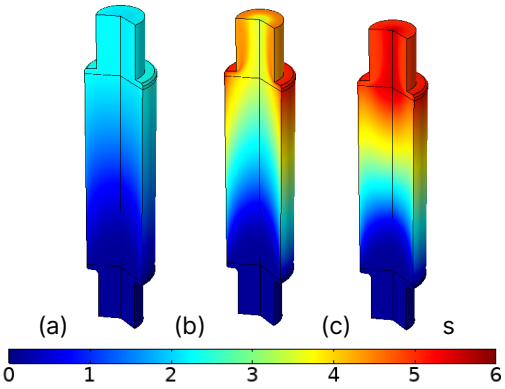

Figure 4. Temporal evolution of NH_3 concentration profiles at key time points. (a) Concentration profile at t = 0.9 s. (b) Concentration profile at t = 1.07 s. (c) Concentration profile at t = 2 s.

Finally, by t=2.0 s, the reactor achieves stabilization, characterized by a uniform NH_3 concentration distribution across the core of the reactor. This indicates that the system has reached a new dynamic equilibrium at the elevated temperature of 430°C. The smooth and rapid stabilization, coupled with a significant increase in NH_3 concentration compared to the initial conditions, demonstrates the reactor's efficiency in managing transient thermal changes. This behavior underscores the role of effective heat transfer and robust catalytic performance in maintaining stability despite fluctuating operating conditions.

These findings validate the transient modeling approach and highlight the reactor's capability to adapt quickly to external thermal disturbances. The results provide valuable insights for optimizing the design and operation of ammonia synthesis reactors in Power-to-Ammonia applications, particularly under the variable conditions imposed by intermittent renewable energy sources.

CONCLUSION

This study developed and validated a 2D axisymmetric transient CFD model to analyze the dynamic response of a fixed-bed ammonia synthesis reactor under thermal perturbations. The results demonstrate a significant enhancement in NH_3 concentration (2.2 to 5.1 vol.%) following a temperature step increase from 400°C to 430°C, with rapid stabilization within 0.5 s. The kinetic advantage of Ru/C catalysts at moderate temperatures was found to outweigh thermodynamic limitations, contributing to increased ammonia production. Spatial temperature distributions exhibited consistent heat transfer patterns, maintaining ~400K differentials between inlet and maximum temperature zones.

Future work will address the broader impact of process conditions by extending the sensitivity analysis to include variations in pressure, gas composition, and flow rates. Additionally, a comparative evaluation of alternative reactor configurations and catalyst materials is under investigation to contextualize the advantages and trade-offs of the proposed system. Further assessment of industrial feasibility and scalability, including potential challenges in commercial implementation, will be explored to enhance the model applicability for Power-to-Ammonia applications. These ongoing efforts aim to refine the predictive capabilities of the model and provide deeper insights for optimizing ammonia synthesis under dynamic operating conditions

ACKNOWLEDGEMENTS

This project is funded by Ministry of Science, Technology, and Innovation (Minciencias, Patrimonio Autónomo del FONDO NACIONAL DE FINANCIAMIENTO PARA LA CIENCIA, LA TECNOLOGÍA Y LA INNOVACIÓN, FRANCISCO JOSÉ DE CALDAS) through the contract 441-2023 and Universidad de La Sabana through the project ING-284-2021. Bravo also acknowledges the support of Universidad de La Sabana through his research assistant position.

NOMENCLATURE

Latin letters

p	pressure, [Pa]
Q	heat rate per unit volume, [W m-3]
t	time, [s]
T	temperature, [K]
$\mathbf{u}$	fluid velocity vector, [-]
$\mathbf{j}$	mass flux, [kg m-2 s-1]

$\mathbf{q}$	heat flux, [W m-2]
$\mathbf{I}$	identity matrix, [-]
R	molar reaction rate, [mol gcat-1 s-1]
M_n	molar mass, [g mol-1]
D_i^m	mixture-average diffusion coefficient, [m^2 s-1]
k_{eff}	effective thermal conductivity of the porous medium, [K m-1 K-1]
C_p	specific heat capacity, [J kg-1 K-1]

Greek letters

ρ	density, [kg m-3]
ω_i	species mass fraction, [-]
μ	fluid dynamic viscosity, [Pa s]
ε_p	catalyst bed porosity. [-]
κ	heat transport coefficient, [W m-1 K-1]
θ	void fraction, [-]
[–]	refers to without units or to dimensionless

Superscripts

m	mixture
T	Transpose operator

Subscripts

i	chemical species: {N2, H2, NH3}
eff	effective

Abbreviations

CFD	Computational Fluid Dynamic
GHSV	Gas Hourly Space Velocity

REFERENCES

1. P. Berwal, S. Kumar, and B. Khandelwal, "A comprehensive review on synthesis, chemical kinetics, and practical application of ammonia as future fuel for combustion," *Journal of the Energy Institute*, vol. 99, pp. 1743–9671, 2021, doi: 10.1016/j.joei.2021.10.001.
2. A. G. Dixon and B. Partopour, "Computational Fluid Dynamics for Fixed Bed Reactor Design," *Annu Rev Chem Biomol Eng*, vol. 11, no. 1, 2020, doi: 10.1146/annurev-chembioeng-092319-075328.
3. M. Tyrański, J. M. Bujalski, W. Orciuch, and Ł. Makowski, "Computational Fluid Dynamics of Ammonia Synthesis in Axial-Radial Bed Reactor," *Energies 2023, Vol. 16, Page 6680*, vol. 16, no. 18, p. 6680, Sep. 2023, doi: 10.3390/EN16186680.
4. I. Rossetti, N. Pernicone, F. Ferrero, and L. Forni, "Kinetic study of ammonia synthesis on a promoted Ru/C catalyst," *Ind Eng Chem Res*, vol. 45, no. 12, 2006, doi: 10.1021/ie051398g.
5. D. C. Dyson and J. M. Simon, "A kinetic expression with diffusion correction for ammonia synthesis on industrial catalyst," *Industrial and Engineering Chemistry Fundamentals*, vol. 7, no. 4, pp. 605–610, Nov. 1968, doi: 10.1021/I160028A013/ASSET/I160028A013.FP.PNG_V03.
6. A. Tripodi, M. Compagnoni, E. Bahadori, and I. Rossetti, "Process simulation of ammonia synthesis over optimized Ru/C catalyst and multibed Fe + Ru configurations," *Journal of Industrial and Engineering Chemistry*, vol. 66, 2018, doi: 10.1016/j.jiec.2018.05.027.
7. T. Gu, S. S. Araya, C. Yin, and V. Liso, "Exploring decentralized ammonia synthesis for hydrogen storage and transport: A comprehensive CFD investigation with experimental validation and parametric study," *Energy Convers Manag*, vol. 295, p. 117604, Nov. 2023, doi: 10.1016/J.ENCONMAN.2023.117604.

© 2025 by the authors. Licensed to PSEcommunity.org and PSE Press. This is an open access article under the creative commons CC-BY-SA licensing terms. Credit must be given to creator and adaptations must be shared under the same terms. See https://creativecommons.org/licenses/by-sa/4.0/